

Nonclassical polarization dynamics in classical-like states

Alfredo Luis^{*,a}, Ángel S. Sanz^b

^a*Departamento de Óptica, Universidad Complutense de Madrid, 28040 Madrid, Spain*

^b*Instituto de Física Fundamental (IFF-CSIC), Serrano 123, 28006 Madrid, Spain*

Abstract

Quantum polarization is investigated by means of a trajectory picture based on the Bohmian formulation of quantum mechanics. Relevant examples of classical-like two-mode field states are thus examined, namely Glauber and SU(2) coherent states. Although these states are often regarded as classical, the analysis here shows that the corresponding electric-field polarization trajectories display topologies very different from those expected from classical electrodynamics. Rather than incompatibility with the usual classical model, this result demonstrates the dynamical richness of quantum motions, determined by local variations of the system quantum phase in the corresponding (polarization) configuration space, absent in classical-like models. These variations can be related to the evolution in time of the phase, but also to its dependence on configurational coordinates, which is the crucial factor to generate motion in the case of stationary states like those here considered. In this regard, for completeness these results are compared those obtained from nonclassical $N00N$ states.

Key words: Light polarization, Glauber states, SU(2) coherent states, $N00N$ states, polarization trajectory, Bohmian mechanics

PACS: 03.65.Ta, 42.25.Ja, 42.50.Ar, 42.50.Xa, 03.50.De

1. Introduction

According to its standard definition [1], light polarization refers to the ellipse described in time by the real component of the electric-field vector

*Corresponding author

Email address: alluis@fis.ucm.es (Alfredo Luis)

of a harmonic wave. Hence partial polarization can then be understood as the rapid and random succession of more or less different polarization states. In the quantum realm, we find that the electric field can never display a well-defined ellipse, just in the same way that particles cannot follow definite trajectories [2]. This is because the (field) quadratures satisfy the same commutation relations of position and linear momentum, and brings in several remarkable consequences: (i) there is no room for the classic, textbook definition of polarization, (ii) the simple and elegant picture of partial polarization as a random succession of definite ellipses gets lost, and (iii) any quantum light state is partially polarized because of unavoidable (quantum) fluctuations. The purpose of this work is to investigate whether these inconvenient quantum consequences can be overcome resorting to the Bohmian picture of quantum mechanics.

Polarization is a preferential laboratory for the analysis and application of fundamental aspects of the quantum theory. In this regard, one can get profit from tools coming from the latter to analyze optical behaviors. This is the case, for instance, when we consider the Bohmian formulation of quantum mechanics [3], which allows us to introduce suitable well-defined trajectories into the domain of quantum optics without violating any fundamental principle. Bearing this in mind, here we address the question of whether the set of trajectories determined by the Bohmian picture can still provide a reliable representation of polarization for quantum light states as an ensemble of electric-field trajectories. This would provide us with a rather intuitive model to understand quantum light closer to the original idea of polarization.

Recently, the trajectories described by the electric field of one-photon two-mode states were determined by following this approach [4]. Here we extend the analysis to more relevant examples of classical-like two-mode field states, namely as Glauber and SU(2) coherent states [5, 6]. Specifically, we focus on this kind of states because a priori one might naively expect that they would constitute the appropriate arena to disclose the statistical description of polarization we are looking for. Surprisingly, we have found that for all these examples of classical-like light the electric-field trajectories are clearly incompatible with classical electrodynamics. Actually, for the SU(2) states we have found that they are far away from even resembling ellipses. For completeness, these results are compared to the polarization trajectories associated with highly nonclassical stationary field, such as $N00N$ states.

This work has been organized as follows. In Section 2 we present the prescriptions to define polarization trajectories as well as a discussion on

the influence of singular points on the polarization dynamics. The dynamics associated with the polarization trajectories for coherent, classical-like states are reported and discussed in Section 3, while in Section 4 we deal with the counterpart for nonclassical, $N00N$ states. To conclude, a series of final remarks are summarized in Section 5.

2. Polarization trajectories

2.1. Polarization guidance equation

In analogy to the Bohmian formulation of quantum mechanics or, in short, Bohmian mechanics [3], polarization trajectories described by the transverse electric field for two-mode harmonic light can be obtained by solving the guidance equation¹

$$\dot{\mathbf{E}} = \nabla S, \quad (1)$$

where $\mathbf{E} = (E_x, E_y)$ denote the real, transverse components of the electric-field strength in Cartesian coordinates, S is the phase of the field-state wave function in quadrature representation, and the gradient ∇S is taken with respect to $\mathbf{E} = (E_x, E_y)$. Notice that, as in the usual Bohmian formulation, we have recast the electric field wave function in polar form,

$$\psi(\mathbf{E}, t) \equiv \langle \mathbf{E} | \psi(t) \rangle = |\psi(\mathbf{E}, t)| e^{iS(\mathbf{E}, t)}, \quad (2)$$

where we have assumed the field state $|\psi(t)\rangle$ to be pure, and $|\mathbf{E}\rangle$ represents the eigenstates of the real part of the complex amplitude operators \hat{a}_k ($k = x, y$), i.e., $\hat{E}_k |\mathbf{E}\rangle = \mathbf{E} |\mathbf{E}\rangle$, with

$$\hat{E}_k = \frac{1}{\sqrt{2}} \left(\hat{a}_k + \hat{a}_k^\dagger \right). \quad (3)$$

Notice that because light polarization just describes the time-evolution of the electric field, its configuration space is given by the electric-field variables (E_x, E_y) , which play the same role as the coordinates \mathbf{r} in the case of particle dynamics. Once the general guidance equation is established, sets of polarization trajectories are determined by plugging the corresponding quantum field state (its phase) into this equation, and then solving it for some particular set of initial conditions, as in classical mechanics.

¹Throughout this work we have considered units such that both field frequency and reduced Planck constant are unity.

It is worth pointing out that in the quantum case all the information about the polarization state is encoded in the scalar wave function $\psi(\mathbf{E}, t)$. More importantly, since $\psi(\mathbf{E}, t)$ represents a probability amplitude, its phase has no classical analog. Therefore all about the polarization trajectories relies on a nonclassical object, and hence we should expect that most conclusions derived from the phase of $\psi(\mathbf{E}, t)$ will have no classical counterpart at all.

2.2. Equilibrium points

Except for the Glauber coherent states, here we have essentially focused on stationary states, and hence the topology of their phase in the polarization configuration space is going to be time-independent. This means that any motion will be associated to this topology rather to the time-evolution of the phase gradient, as shown in [4]. In this case, the mathematical framework of the stability theory is of much interest, for it may allow us to elucidate dynamical properties by identifying possible equilibrium points [7]. This points are going to determine the behavior of the polarization trajectories in their vicinity and, therefore, the general dynamical landscape associated with each quantum state.

The nodes or zeros of the wave function, where $\psi(\mathbf{E}) = 0$ and the phase S is undefined, constitute the first kind of candidate to equilibrium point. As is well known [8, 9, 10], nodes or phase singularities organize the global spatial structure of the flow of an optical field. This follows from Stoke's theorem, which states that unless the curl of certain vector field is zero within a certain region (irrotational flow), the line integral around a closed loop enclosing such a region (i.e., the circulation of such a vector field) will be nonzero. If this vector field is identified with the phase gradient, then we know that this quantity will be invariant under the addition to the phase of any integer multiple of 2π . Consequently, if the curl of ∇S is nonzero, its circulation will be quantized. This is precisely what we observe in the case of Bohmian trajectories that whirl around a node of the wave function [11, 12], where the quantization is in terms of integer multiples of $2\pi\hbar$. Of course, this also holds for the polarization trajectories that we are dealing with here, since

$$\oint \dot{\mathbf{E}} \cdot d\mathbf{E} = \oint dS = 2\pi q. \quad (4)$$

As it can be inferred from the latter integral, the presence of zeros in the wave function allows the introduction of a circulation number or topological charge, q . This number has to be an integer, since the line integral provides the

change experienced by the phase after an excursion returning to the original point [13, 14, 15, 16]. Or, in topological terms, it accounts for the number of jumps between different equivalent points of the Riemann surface described by the logarithm of the wave function. In all cases examined in this work, the trajectories around the zeros will be nearly circular in a neighborhood of the node, giving rise to a vortical dynamics [11, 12, 13]. It is worth noting that in quantum mechanics, it was Dirac who first noticed this effect [17], suggesting the existence of magnetic monopoles. The concept of magnetic monopole has been further developed in the literature within the grounds of quantum hydrodynamics [18]. On the other hand, recently it has also been possible to recreate in laboratory conditions Dirac's monopoles making use of the properties displayed by different materials, such as crystals made of spin ice [19] or Bose-Einstein condensates of rubidium atoms [20]. Strictly speaking, these are not elementary monopoles, but quasi-particles arising as an emergent phenomenon associated with a collective behavior, which display analogous properties to the hypothesized Dirac monopole.

Critical or stationary points, i.e., points at which all partial derivatives of a given function are zero, constitute the second kind of equilibrium point that we may identify. In our particular context, stationary points \mathbf{E}_s will produce a vanishing phase gradient, i.e., $\nabla S = 0$. That is, given the guidance equation (1), we will find

$$\left. \frac{d^k \mathbf{E}}{dt^k} \right|_{\mathbf{E}=\mathbf{E}_s} = \mathbf{0} \quad (5)$$

for all $k > 0$. In all the cases examined in this work, the trajectories near these points are hyperbolic, with the corresponding value of \mathbf{E}_s being a saddle point of the velocity field ∇S . We have found no maxima or minima of S , which would lead respectively to sinks and sources of trajectories.

It is worth noticing that both nodes and stationary points are zeros of the current density, $\mathbf{j} = |\psi|^2 \nabla S = \text{Im}(\psi^* \nabla \psi)$. Nonetheless, the role played by these two types of equilibrium points is different. The asymptotically stable and unstable branches associated with the stationary points define separatrices around the nodes, which determine domains with different dynamical behavior. In particular, the direction of the flow around the nodes changes the sign when one passes from the domain of one of these nodes to another adjacent one. As it will be seen below, in some cases these domains are included within a larger domain with a preferential flow direction, while in others the full configuration space is totally divided in domains without

enabling the appearance of larger domains.

3. Field trajectories for classical-like states

3.1. Glauber coherent states

Two-mode quadrature coherent states, typically known as Glauber coherent states and denoted as $|\alpha_x, \alpha_y\rangle$, constitute the paradigm of classical light. Their electric-field wave function is just a Gaussian,

$$\psi(\mathbf{E}, t) \propto e^{-(\mathbf{E}-\boldsymbol{\mathcal{E}})^2/2} e^{i\boldsymbol{\mathcal{B}}\cdot\mathbf{E}}, \quad (6)$$

where $\boldsymbol{\mathcal{E}}$ and $\boldsymbol{\mathcal{B}}$ are real two-dimensional vectors defined according to the relation $\sqrt{2}\boldsymbol{\alpha}e^{-it} = \boldsymbol{\mathcal{E}} + i\boldsymbol{\mathcal{B}}$, being $\boldsymbol{\alpha} = (\alpha_x, \alpha_y)$. Thus these vectors evolve in time as

$$\boldsymbol{\mathcal{E}}_k = \sqrt{2}|\alpha_k| \cos(t - \delta_k), \quad \boldsymbol{\mathcal{B}}_k = -\sqrt{2}|\alpha_k| \sin(t - \delta_k), \quad (7)$$

with $\delta_k = \arg \alpha_k$ for $k = x, y$. Since the phase is $S = \boldsymbol{\mathcal{B}} \cdot \mathbf{E}$ the guidance equation is simply $\dot{\mathbf{E}} = \nabla S = \boldsymbol{\mathcal{B}}$, which can be easily solved analytically to give

$$E_k(t) = E_k(0) + \sqrt{2}|\alpha_k| \cos(t - \delta_k) - \sqrt{2}|\alpha_k| \cos \delta_k, \quad (8)$$

this is to say

$$\mathbf{E}(t) - \mathbf{E}(0) = \boldsymbol{\mathcal{E}}(t) - \boldsymbol{\mathcal{E}}(0). \quad (9)$$

In Fig. 1 we have plotted three polarization trajectories for a Glauber coherent state by considering different initial conditions in Eq. (8). The solid line represents the most probable trajectory, starting at $t = 0$ at the maximum of (6), i.e., $\mathbf{E}(0) = \boldsymbol{\mathcal{E}}(0)$ so that $\mathbf{E}(t) = \boldsymbol{\mathcal{E}}(t)$; the other two trajectories (dashed and dotted lines) start from points at one standard deviation from the maximum. The background represents a contour-plot of the probability density associated with the one-cycle averaged probability distribution for the electric field

$$\overline{P}(\mathbf{E}) \propto \int_0^{2\pi} |\psi(\mathbf{E}, t)|^2 dt. \quad (10)$$

As happens with the Bohmian trajectories of a quantum harmonic oscillator, here we also notice that any trajectory associated with a Glauber state displays the same topology and keeps a constant distance with respect to the most probable one, as it is inferred from Eq. (9). In this case, this topology coincides with the polarization ellipse of a classical harmonic wave with

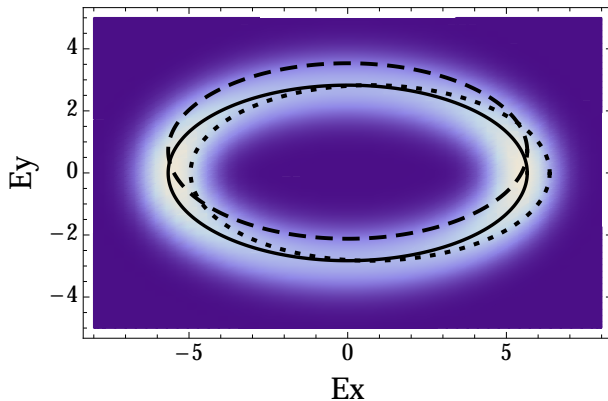


Figure 1: Polarization trajectories for a two-mode coherent state with $\alpha_x = 4$ and $\alpha_y = 2i$. The contour-plot represents the probability density associated with the one-cycle averaged probability distribution for the electric field $\bar{P}(\mathbf{E})$.

complex-amplitude vector $\boldsymbol{\alpha}$. Nonetheless, only the most probable trajectory (the solid line in Fig. 1) is centered at the origin; any other trajectory will be slightly displaced, as mentioned before (see dashed and dotted lines in Fig. 1). Despite coherent states are regarded as typical examples of classical-like light, such a displacement constitutes an important difference with respect to what one would expect from classical electrodynamics, namely zero displacement (i.e., concentric trajectories).

3.2. $SU(2)$ coherent states

The two-mode Glauber coherent states define another interesting family of classical-like states regarding polarization, namely the $SU(2)$ coherent states. These states arise after recasting the two-mode Glauber coherent states as [6]

$$|\alpha_x, \alpha_y\rangle = e^{-|\alpha|^2/2} \sum_{n=0}^{\infty} \frac{\alpha^n e^{in\delta}}{\sqrt{n!}} |n, \Omega\rangle. \quad (11)$$

Here $|n, \Omega\rangle$ denotes the $SU(2)$ coherent state with n photons, which reads explicitly as

$$|n, \Omega\rangle = \sum_{k=0}^n \binom{n}{k}^{1/2} \cos^k \frac{\theta}{2} \sin^{n-k} \frac{\theta}{2} e^{-ik\delta} |k, n-k\rangle, \quad (12)$$

where $|k, n - k\rangle$ are two-mode photon-number states, and

$$\alpha_x = \alpha \cos \frac{\theta}{2}, \quad \alpha_y = \alpha \sin \frac{\theta}{2} e^{-i\delta}. \quad (13)$$

It is worth noting that the polarization state, as given by the Stokes parameters, is the same for the Glauber coherent states and all the SU(2) coherent states in Eq. (11).

The wave function $\psi(\mathbf{E}, t)$ accounting for SU(2) coherence states with n photons, given by Eq. (12), reads as

$$\psi(\mathbf{E}, t) \propto \sum_{k=0}^n \frac{\alpha_x^k \alpha_y^{n-k}}{k!(n-k)!} H_k(E_x) H_{n-k}(E_y) e^{-\mathbf{E}^2/2} e^{-int}, \quad (14)$$

where we have considered the fact that in the electric-field quadrature representation

$$\langle E_x, E_y | n_1, n_2 \rangle = \frac{H_{n_1}(E_x) H_{n_2}(E_y)}{\sqrt{2^{n_1+n_2} \pi n_1! n_2!}} e^{-\mathbf{E}^2/2}, \quad (15)$$

with H_n representing the Hermite polynomials.

Here, the only analytical solution to the guidance equation holds in the particular case of $|\alpha_x| = |\alpha_y|$ and $\delta = \pm\pi/2$, for which we have $\psi(\mathbf{E}) \propto (E_x \pm iE_y)^n e^{-\mathbf{E}^2/2}$. In this case, all trajectories are circles and there is only one node at the origin with charge $q = \pm n$, the sign depending on the helicity of the classical polarization ellipse.

This coincides exactly with the circular polarization associated with the complex-amplitude vector $\boldsymbol{\alpha}$. For any other general case, the trajectories shown in the top panel of Fig. 2 provide an idea of the general trend. These trajectories, displayed in the form of streamlines (arrows indicate the directionality of the motion), correspond to an SU(2) coherent state with $\alpha_x = 4$, $\alpha_y = 2i$, and $n = 3$; the contour-plot represents the probability density $|\psi(\mathbf{E}, t)|^2$ associated with the coherent state considered. This example illustrates without loss of generality the results we have found for all cases examined, specifically that there are n nodes located along the major axis of the classical ellipse associated with the complex vector $\boldsymbol{\alpha}$. In the vicinity of the nodes, the trajectories are nearly circular [13], as can be better seen in the enlargement around the central node provided in the central panel of Fig. 2. The three nodes have the same topological charge $q = +1$. Between any two consecutive nodes, along the line connecting them, there are $n - 1$

hyperbolic stationary points [7]. In the vicinity of these points, the trajectories display a hyperbolic topology with identical semi-axes (see central panel in Fig. 2).

The trajectory that passes just through the two stationary points is a separatrix, which separates the three dynamical domains associated with each node from a single outer domain, where the trajectories move around the all three nodes. Actually, far from the nodes the trajectories tend to be circular. This can be readily shown analytically by considering the approximation $H_n(x) \approx (2x)^n$ for large x , and substituting it into the wave function (14), which yields

$$\psi(\mathbf{E}) \propto (\boldsymbol{\alpha} \cdot \mathbf{E})^n e^{-\mathbf{E}^2/2}, \quad (16)$$

and hence $\dot{\mathbf{E}} \propto (E_y, -E_x)$, $\dot{\mathbf{E}}\mathbf{E} = 0$, and $|\mathbf{E}| = \text{constant}$ along each trajectory, which define a circular motion. Of course, the rotation of the outer trajectories the three central domains can be associated with the motion around a single effective node of charge $q = +3$. As an illustration of the extremely streaking behavior displayed by the associated polarization trajectories in the case of these classical-like polarization states is given by the set of trajectories shown in the bottom panel of Fig. 2. As is apparent, they are all clearly incompatible with the classical electrodynamics corresponding to a freely evolving two-mode harmonic electric field.

4. Nonclassical field: $N00N$ states

For the sake of comparison, we will also briefly consider a paradigmatic case of nonclassical state, namely a $N00N$ state. These states constitute the polarization analog of Schrödinger cat states or coherent superpositions of distinguishable states. In the photon-number basis they read [24] as

$$|\psi\rangle \propto \alpha_x |n, 0\rangle + \alpha_y |0, n\rangle. \quad (17)$$

This can be regarded as an alternative quantum version of the coherent superposition of two orthogonal oscillations, which is the actual origin of polarization. The corresponding wave function is

$$\psi(\mathbf{E}) \propto [\alpha_x H_n(E_x) + \alpha_y H_n(E_y)] e^{-\mathbf{E}^2/2}. \quad (18)$$

A global picture of the dynamics for $N00N$ states is provided in Fig. 3 (left) in terms of streamlines. To compare with the case analyzed in Section 3, the values $\alpha_x = 4$, $\alpha_y = 2i$, and $n = 3$ have been considered again.

An enlargement showing the dynamical details in the vicinity of one of the hyperbolic stationary points and the adjacent nodes can be seen in the right panel. The nodes form an array of $n \times n$ domains, where the trajectories are nearly circles with $q = \pm 1$. In this case, the sign of q is always opposite for nearest neighbors. On the other hand, the stationary points form a $(n - 1) \times (n - 1)$ array, such that the corresponding separatrices divide the configuration space into isolated domains regardless of how far we find from the nodes. These points are located along the diagonals connecting nodes with the same sign of q and, again, the trajectories in their vicinity display a hyperbolic topology.

5. Conclusions

We have addressed a Bohmian approach to light polarization in quantum optics by computing the trajectories described by the electric field of some classical-like two-mode states. For Glauber coherent states all trajectories have the same elliptic form of the mean field, although they are not centered at the origin. For $SU(2)$ coherent states, trajectories are even further away from being ellipses. This may be ascribed to the fact that $SU(2)$ coherent states are stationary and hence their dynamics must have a purely geometric origin. As we have shown this is largely determined by the equilibrium points of the electric-field wave function. We have also shown that this geometrical nature is also displayed in a similar fashion by nonclassical light.

These results are in contradiction to classical electrodynamics. This is quite remarkable since these field states are universally regarded as classical-like concerning polarization. Nonetheless, there are some quantum approaches where these states may also display nonclassical polarization features as discussed in [21]. In this regard, it is worth noticing that the definition of the electric-field trajectories has no straightforward classical counterpart, since there seems to be no simple classical version of the phase of the electric-field wave function.

Acknowledgements

Support from the Ministerio de Economía y Competitividad (Spain) under Projects Nos. FIS2012-35583 (AL) and FIS2011-29596-C02-01 (AS) as well as a “Ramón y Cajal” Research Fellowship with Ref. RYC-2010-05768 (AS), and the Consejería de Educación de la Comunidad de Madrid under Project No. QUITEMAD S2009-ESP-1594 (AL).

References

- [1] M. Born, E. Wolf, Principles of Optics, Cambridge University Press, Cambridge, 1999, 7th ed.
- [2] S. De Bièvre, J. Phys. A 25 (1992) 3399–3418;
J. Pollet, O. Méplan, C. Gignoux, J. Phys. A 28 (1995) 7287–7297;
A. Luis, Phys. Rev. A 66 (2002) 013806(1–8);
J. Liñares, M.C. Nistal, D. Barral, V. Moreno, Eur. J. Phys. 31 (2010) 991–1005;
J. Liñares, D. Barral, M.C. Nistal, V. Moreno, J. Mod. Opt. 58 (2011) 711–725.
- [3] A.S. Sanz, S. Miret-Artés, A Trajectory Description of Quantum Processes. I. Fundamentals, Springer, Berlin, 2012.
- [4] A. Luis, A.S. Sanz, Phys. Rev. A 87 (2013) 063844(1–8).
- [5] L. Mandel, E. Wolf, Optical Coherence and Quantum Optics, Cambridge University Press, Cambridge, UK, 1995;
O. Giraud, P. Braun, D. Braun, Phys. Rev. A 78 (2008) 042112(1–9).
- [6] P.W. Atkins, J.C. Dobson, Proc. R. Soc. Lond. A 321 (1971) 321–340;
F.T. Arecchi, E. Courtens, R. Gilmore, H. Thomas, Phys. Rev. A 6 (1972) 2211–2237.
- [7] D.W. Jordan, P. Smith, Nonlinear Ordinary Differential Equations, Oxford University Press, Oxford, 1999, 3rd Ed.
- [8] M.V. Berry, Singularities in Waves, in Les Houches Lecture Series Session XXXV, eds. R. Balian, M. Kléman, J.-P. Poirier, North-Holland, Amsterdam, 1981, pp. 453–543.
- [9] M.V. Berry, Wave Geometry: A plurality of singularities, in *Quantum Coherence*, ed. J.S. Anandan, World Scientific, New York, 1991, pp. 92–98.
- [10] M.V. Berry, M.R. Dennis, Proc. R. Soc. A 457 (2001) 141–155.
- [11] J.O. Hirschfelder, A.C. Christoph, J. Chem. Phys. 61 (1974) 5435–5455;
J.O. Hirschfelder, Ch.J. Goebel, L.W. Bruch, J. Chem. Phys. 61 (1974) 5456–5459.

- [12] A.S. Sanz, F. Borondo, S. Miret-Artés, *Phys. Rev. B*, 69 (2004) 115413(1–5);
A.S. Sanz, F. Borondo, S. Miret-Artés, *J. Chem. Phys.* 120 (2004) 8794–8806.
- [13] M.V. Berry, *J. Phys. A* 38 (2005) L745–L751.
- [14] E. Merzbacher, *Am. J. Phys.* 30 (1962) 237–247.
- [15] J. Riess, *Phys. Rev. D* 2 (1970) 647–653.
- [16] J. Riess, *Phys. Rev. D* 2 (1976) 3862–3869.
- [17] P.A.M. Dirac, *Proc. R. Soc. Lond. A* 133 (1931) 60–72.
- [18] I. Białynicki-Birula, Z. Białynicka-Birula, *Phys. Rev. D* 3 (1971) 2410–2412.
- [19] D.J.P. Morris, D.A. Tennant, S.A. Grigera, B. Klemke, C. Castelnovo, R. Moessner, C. Czternasty, M. Meissner, K.C. Rule, J.-U. Hoffmann, K. Kiefer, S. Gerischer, D. Slobinsky, R.S. Perry, *Science* 326 (2009) 411–414
T. Fennell, P.P. Deen, A.R. Wildes, K. Schmalzl, D. Prabhakaran, A.T. Boothroyd, R.J. Aldus, D.F. McMorrow, S.T. Bramwell, *Science* 326 (2009) 415–417;
S.T. Bramwell, S.R. Giblin, S. Calder, R. Aldus, D. Prabhakaran, T. Fennell, *Nature* 461 (2009) 956–959;
H. Kadowaki, N. Doi, Y. Aoki, Y. Tabata, T.J. Sato, J.W. Lynn, K. Matsuhira, Z. Hiroi, *J. Phys. Soc. Jpn.* 78 (2009) 103706(1–4).
- [20] M.W. Ray, E. Ruokokoski, S. Kandel, M. Möttönen, D.S. Hall, *Nature* 505 (2014) 657–660;
For completeness, see also the theoretical companion article: V. Pietilä, M. Möttönen, *Phys. Rev. Lett.* 103 (2009) 030401(1–4).
- [21] A. Luis, *Phys. Rev. A* 73 (2006) 063806(1–10);
L.M. Johansen, *Phys. Lett. A* 329 (2004) 184–187;
L.M. Johansen, A. Luis, *Phys. Rev. A* 70 (2004) 052115(1–12).
- [22] J. Schwinger, *Quantum Theory of Angular Momentum*, Academic Press, New York, 1965.

- [23] R. Delbourgo, *J. Phys. A* 10 (1977) 1837–1846.
- [24] N.D. Mermin, *Phys. Rev. Lett.* 65 (1990) 1838–1840;
J.J. Bollinger, W.M. Itano, D.J. Wineland, D.J. Heinzen, *Phys. Rev. A* 54 (1996) R4649–R4652;
Ph. Walther, J.-W. Pan, M. Aspelmeyer, R. Ursin, S. Gasparoni, A. Zeilinger, *Nature* 429 (2004) 158–161;
M.W. Mitchell, J.S. Lundeen, A.M. Steinberg, *Nature* 429 (2004) 161–164.
- [25] M.R. Dennis, K. O’Holleran, M.J. Padgett, *Prog. Opt.* 53 (2009) 293–363.

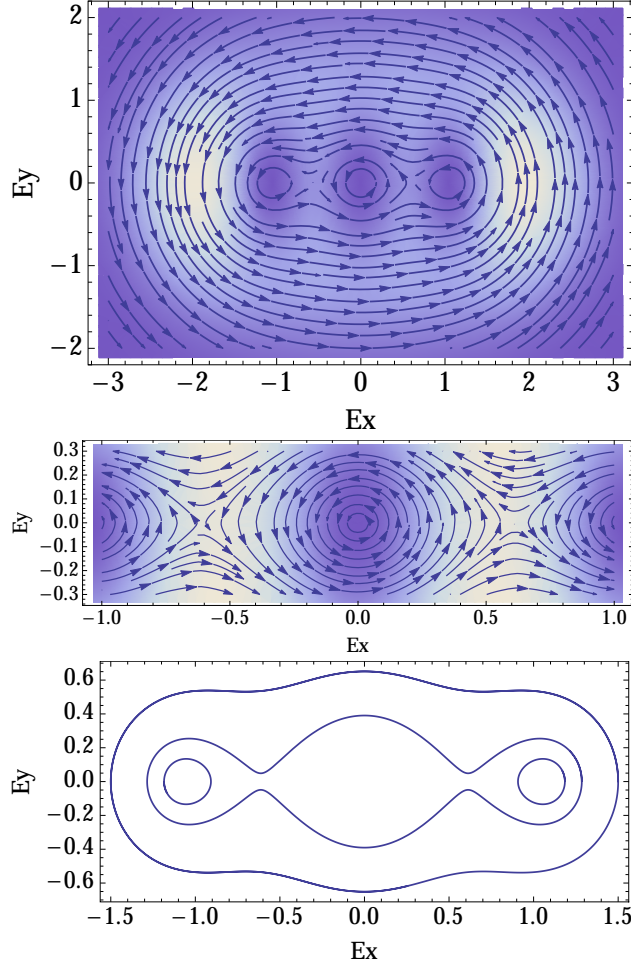


Figure 2: Top: Streamlines illustrating the trajectory dynamics associated with an $SU(2)$ coherent state with $\alpha_x = 4$, $\alpha_y = 2i$, and $n = 3$. The contour-plot represents the probability density $|\psi(\mathbf{E}, t)|^2$ of the electric-field. Middle: Enlargement of the upper panel to show the dynamics around the central node and the two adjacent hyperbolic stationary points. Bottom: Four polarization trajectories showing the incompatibility with the classical electrodynamics of a freely evolving two-mode harmonic electric field.

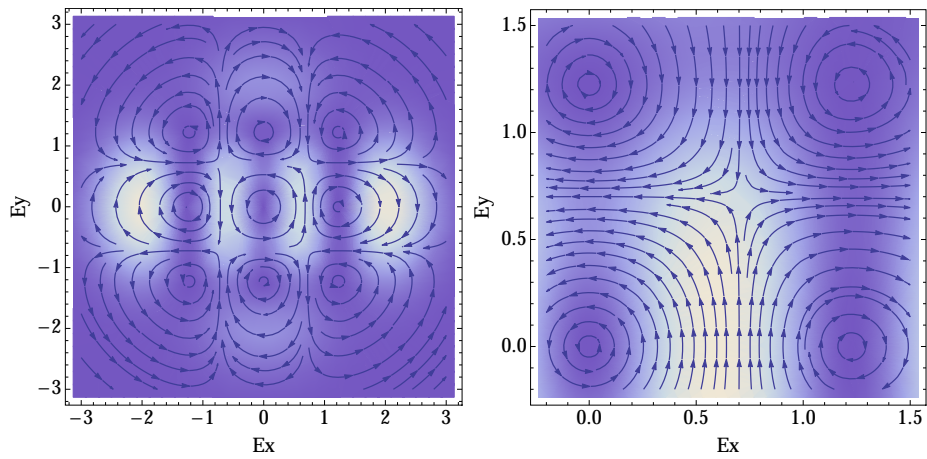


Figure 3: Left: Streamlines illustrating the trajectory dynamics associated with a $N00N$ state with $\alpha_x = 4$, $\alpha_y = 2i$, and $n = 3$. The contour-plot represents the probability density $|\psi(\mathbf{E}, t)|^2$ of the electric-field. Middle: Enlargement of the upper panel to show the dynamics around one of the hyperbolic stationary points and the adjacent nodes.